Received: 3 February 2022 | Revised: 19 January 2023 | Accepted: 25 January 2023

DOI: 10.1111/maec.12741

RESEARCH ARTICLE

marine ecology WILEY

Predicting diversity in benthic macro-scale communities associated with mussel matrices in three Pacific ecoregions

Lynn Wilbur[1] | Frithjof C. Küpper[1,2] | Nikolaos Katsiaras[3] | Vasilis Louca[1]

[1]School of Biological Sciences, University of Aberdeen, Scotland, UK

[2]Marine Biodiscovery Centre, Department of Chemistry, University of Aberdeen, Scotland, UK

[3]Insitute of Oceanography, Hellenic Centre for Marine Research, Greece

Correspondence
Vasilis Louca, School of Biological Sciences, University of Aberdeen, Scotland, UK.
Email: v.louca@abdn.ac.uk

Funding information
Scottish Funding Council, Grant/Award Number: HR09011

Abstract

Marine mussels are ubiquitous and their tough byssal threads allow for the formation of expansive, age-aggregated mats known as mussel matrices which can host marine invertebrates and algal macro-benthic communities playing an important role in food-web dynamics. Yet, despite the significant implications for biodiversity and intertidal ecosystem functioning, the role of mussel size, individual morphology and community arrangement in determining the structure of the associated community has never been investigated. Species representative of the green, brown and red marine algal phyla as well as polychaetes, crustaceans and gastropods were sampled from mussel matrices in the Guayaquil (GUAY), Humboldtian (HWS, HNS) and North American Pacific Fjordland (NAPF) marine ecoregions. Linear mixed effects modelling (LMM) and linear effects modelling (LEM) were used to determine the effect of mussel matrices as a predictor of species diversity by incorporating variability due to ecoregion and sampling site. Shell length and stratum index demonstrated significant effect on species richness (S_{obs}) and Menhinick's richness (D), while stratum index demonstrated an effect on species diversity (H). In the linear mixed model analysis, shell length explained most of the variation in Menhinick's richness (D) and observed species richness (S_{obs}), while stratum index explained most of the variation in (D) in the linear effects model. Our findings reveal that the level of complexity in mussel assemblages plays a major role in determining species diversity.

KEYWORDS
epifaunal community, intertidal zone, species richness, stratum index

1 | INTRODUCTION

1.1 | Background

Marine benthic fauna is highly diverse. Among these, marine mussels are widely abundant and known to form complex beds which can host a diverse assembly of marine fauna and flora (Commito et al., 2008; Günther, 1996; Jaramillo et al., 1992). Nevertheless, species composition of these epifaunal communities on mussel beds is known to vary considerably between locations, even when the same mussel species forms the substratum (Hammond & Griffiths, 2006; Lee & Castilla, 2012). It is established that some of this variability in species composition and observed diversity patterns is due to their position in the intertidal zone (Thiel & Ullrich, 2002). On a bigger geographical scale, latitude seems to drive variability in epifaunal diversity between similar mussel beds (Sepúlveda et al., 2016), with depth also being an important factor, often observing epifaunal diversity levels increasing with increasing depth (Buhl-Mortensen

et al., 2010). On the contrary, some studies even seem to suggest that the faunal abundance associated with mussel beds is independent of mussel bed structure or species composition (Hammond & Griffiths, 2006). The majority of studies though suggest that mussel bed identity and characteristics do influence levels of epifaunal diversity (Cole, 2009; Kelaher, 2003). Specifically, mussel bed geometry is known to influence ecosystem function (Commito et al., 2014; Paquette et al., 2019), but, to date, few studies have focused specifically on the relationship between mussel bed geometry and species diversity and none have specifically dealt with the characteristics and relationship between mussel bed geometry and species diversity, which this study focuses on. Furthermore, developing an understanding of how the mussel bed structure influences diversity in different marine ecoregions is also of importance, especially when taking into account the demonstrated impact of latitude on epifaunal community characteristics (Sepúlveda et al., 2016).

1.2 | Mussel stratum index

Mussels are limited by space and food availability with the problem of space mitigated through mussel layering, also known as the mussel matrix. Guiñez and Castilla (1999) have derived a simple mathematical method for assigning a stratum index to mussel samples based on the height of the sampled mussel bed, the length of the shell, the area of the sampled matrix and the total area that would be covered by mussels if they formed a monolayer. Their model is derived from the research on predicting mussel matrix volume and area by Hosomi (1985). In this study, we model the relationship between species richness in the mussel communities under study using linear mixed effects modelling with the objective of identifying a biomarker of species richness for the ecoregions under study, where shell length, matrix depth and stratum index are the fixed effects and site and ecoregion are the random effects. Furthermore, we consider the practical use of matrix depth versus stratum index as a field application for differentiating matrix layers and for determining species richness.

A comprehensive understanding of these benthic macro-scale communities as they relate to mussel assemblages may provide a framework for coastal management (Bateman & Bishop, 2017; Engle, 2008). This study was conducted with the primary aim of understanding the role of mussel size and mussel matrix structure on benthic macro-scale community diversity and richness in different marine ecoregions.

2 | MATERIALS AND METHODS

2.1 | Study site and ecoregions

The current study borrows from the Census of Marine Life's concept of mapped classifications of marine areas (Marine Ecoregions of the World (MEOW) – Census of Marine Life Maps and Visualization 2010) and put forward by Spalding et al. (2007) for the purpose of representing ecologically important coastal areas for comparisons on multiple geographic scales. Spalding et al. (2007) comprised a list of definitions of the classification system that is parallel to the classification established by the International Union for the Conservation of Nature (Fosberg, 1976), which ranges from largest in scale to smallest consisting of Realms, Provinces and Ecoregions. All of the ecoregions included in this study contain mussel species that are broadly endemic to each Province. The ecoregions under consideration include the North American Fjordland (NAPF) between ~50° and 59° N, the Guayaquil (GUAY) ecoregion between ~0° and 6° S and the Humboldtian ecoregion between ~12° and 26° S (Figure 1).

In order to increase the spatial resolution of the Humboldtian ecoregion, two divisions are proposed based on the width of the continental margin: the Humboldtian wide-shelf (HWS) ecoregion between 12° S and 13° S is approximately 225 km from the edge of the continental shelf to the coastline; and the Humboldtian narrow-shelf (HNS) ecoregion between 15° S and 16° S, and 23° S and 24° S, with a continental shelf approximately half that of the HWS (Krabbenhöft et al., 2004; Strub, 1998). Four sites within the NAPF ecoregion, three sites within the HWS ecoregion and five sites within the HNS ecoregion were chosen based on the presence of endemic mussel species (Figure 1). The focus on areas with endemic mussel species was to ensure that the epifaunal communities and diversity patterns will better reflect the natural state of these ecoregions. Geographic coordinates for the NAPF, GUAY, HWS, and HNS ecoregions and sites within those ecoregions are shown in Table 1. Mussel plots were selected at each site where mussels were present in the high-to-low intertidal zone. A minimum of 5 replicate plots with a minimum of 20% coverage of a 70 × 50 cm quadrat were chosen either along a transect vertical to the waterline or where mussels formed narrow but continuous bands. Where it was possible to sample the same site, care was taken to not re-sample the same quadrats by marking the location of each sampled assemblage using a reel transect. The total number of replicate quadrats (n) by ecoregion is shown in Table 2. Mussel plots were sampled in the GUAY ecoregion, in the HWS ecoregion and at Reserva Punta San Juan (PSJ) in the HNS ecoregion in the austral summer of 2017, mussel plots were sampled at one new site in the HNS ecoregion in 2018 and additional mussel plots were sampled at the PSJ site in the HNS ecoregion in 2019. Mussel plots at sites within the NAPF ecoregion were sampled separately in the boreal summers of 2017 and 2018. No re-sampling of any of the plots occurred during any of the sampling events.

2.2 | Mussel species and macrofaunal sampling

The two most commonly found species of mussels (family Mytelidae) in the Humboldtian ecoregion are *Perumytilus purpuratus* (Lamarck 1819) and *Semimytilus algosus* (Gould 1850), with *Brachidontes* spp. as the dominant genus north of 5 degrees latitude in the GUAY ecoregion (L. Wilbur unpubl. data). *P. purpuratus* and *S. algosus* are associated with high biodiversity and are thus

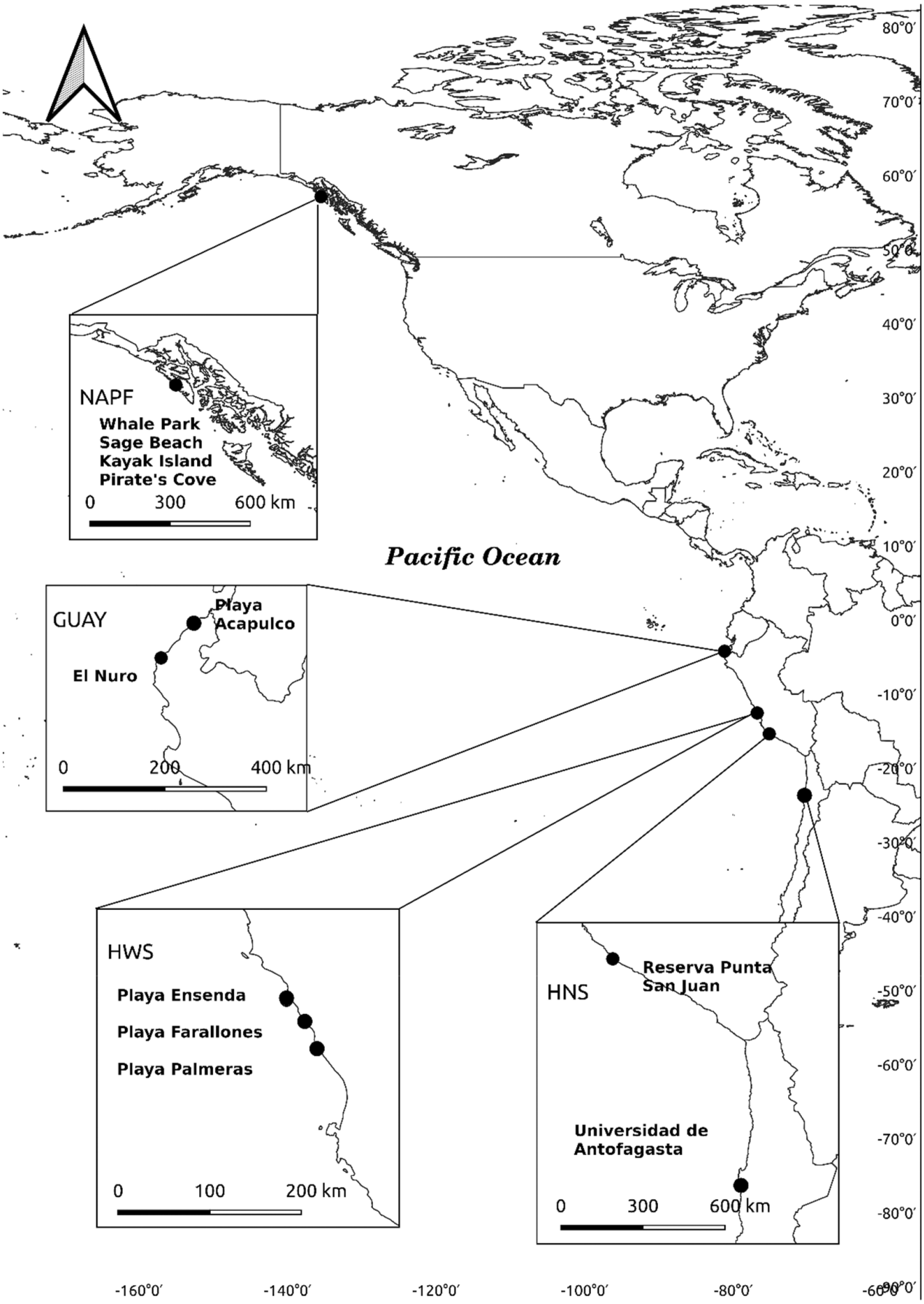

FIGURE 1 Overview map of the western portion of the northern and southern hemispheres in the eastern Pacific and associated ecoregions (insets) and the study sites (black dots) where mussel plots were sampled.

considered to be "bioengineer" species (Jones et al., 1997; Prado & Castilla, 2006). In Peru, *P. purpuratus* is found in the mid-to-low intertidal zone while *S. algosus* is typically found overlapping with *P. purpuratus* in the mid zone, becoming abundant and the predominant mussel species in the low zone, with some spatial overlap between the two species (Tokeshi & Romero, 2000). Assemblages of *P. purpuratus* and *S. algosus* were the targets for measuring abundances of invertebrates and algae that exist as microcosms within the mussel assemblages at Playa Ensenada, Playa Farallones and Playa Palmeras respectively.

TABLE 1 Geographic coordinates for all ecoregions, sub-ecoregions within ecoregions, and sites within ecoregions and sub-ecoregions where mussel assemblages were sampled for this study.

Ecoregion/site	Latitude	Longitude
Guayaquil (GUAY)	~0°S to 3°S	
Humboldtian	~12°S to 26°S	
Humboltdian Wide-Shelf (HWS)	12°37'S to 12°58'S	75°11'W to 76°40'W
Playa Ensendada (PEN)	12°38'S	76°40'S
Playa Farallones (PFA)	12°44'S	76°37'51W
Playa Palmeras (PGA)	12°57'56S	76°30'W
Humboldtian Narrow-Shelf (HNS)	15°21'S to 23'S	70'W to 75°11'W
Reserva Punta San Juan (PSJ)	15°18'S	75°11'W
Universidad de Antofagasta (UOA)	23°42'S	70°25'27,
North American Pacific Fjordland (NAPF)	~50°N to 59°N	
Whale Park	57° 1'57.72"N	135°15'1.08"W
Kayak Island	57°0'30.42"N	135°21'11.16"W)
Sage Beach	57°3'30.348"N	135°19'21.36"W)
Pirate's Cove	56°59'13.2"N	135°22'42.96"W)

In the NAPF ecoregion, two species of mussels found in the intertidal zone are *Mytilus trossulus* and *Mytilus californianus*, with the introduced species *Mytilus galloprovincialis* and *Mytilus edulis* reported for the Pacific Northwest. *M. trossulus* is typically found in concentrated assemblages well above the zero-foot tidal height assigned to the mean low water soundings, whereas *M. californianus* typically occurs in stands of one to few individuals well below the zone where assemblages of *M. trossulus* are found (L. Wilbur, unpublished data). As *M. edulis* and *M. galloprovincialis* occur in intertidal areas in Sitka Sound alongside stands of *M. trossulus*, identification between the species using shell morphology technique is not considered reliable (Hilbish et al., 2002); therefore, a consideration of the *M. edulis/trossulus/galloprovincialis* complex has been suggested when designating species identification in the field in the absence of genetic analysis and mussels from the NAPF ecoregion will be referred henceforth as MYTCOM.

Intertidal assemblages associated with mussel communities were sampled by counting invertebrates and the thalli of algae attached to the outer shells of mussels at each site with a 70×50 cm quadrat strung to provide 10 transects with 100 intersections (Engle, 2008). In order to include algal sporelings and invertebrates that might be missed living below the top layers of mussels, we sub-sampled the quadrat by selecting 10 intersections across the quadrat with a random numbers calculator. First, a plastic Vernier calliper with a retractable stainless-steel rod was inserted into the mussel assemblage to measure the depth of the matrix to the nearest 0.5 mm from the tip of the highest mussel to where the rod touched the rock substrate (Prado & Castilla, 2006). Similar to the methods used by Guiñez and Castilla (1999), mussels were then removed from under each intersection using a 20×60 mm stainless steel spatula to fill a 100 mm^2 frame. The mussel matrices were then placed in a tray and covered with a shallow layer of seawater for approximately 30 min to allow mobile animals to emerge from the shells. Invertebrates and algal sporelings ≥1 mm in length living inside and on the mussels were examined using a hand lens and Nikon field 20x stereoscope and counted. Reference samples were preserved in 70% EtOH (invertebrates) and seawater

TABLE 2 Units of central tendency for (a) fixed effects mean ± SD and range and (b) response variables (median denoted by *) or mean ± SD calculated from mussel plot data pooled for each ecoregion.

	(a) Shell length	Matrix depth	Stratum index	(b) Menhinick's richness (D)	Observed species richness (S_{obs})	Shannon–Wiener diversity
NAPF (n = 35)	22.4 (±4.2)	28.3 (±0.99)	2.8 (±10.5)	1.5 (±0.4)	13.0 (±3.0)	2.0 (±0.3)
	15.3/31.5	14.3/58.0	1.4/5.5	0.1/2.4	7.0/18.0	1.4/2.5
GUAY (n = 11	5.9 (±0.10)	6.1 (±1.4)	1.0 (±0.3)	0.4*	3.0*	1.2 (±0.4)
	4.5/8.0	4.3/8.8	0.7/1.9	0.3/1.1	2.0/10.0	0.7/1.9
HWS (n = 15)	26.4 (±4.7)	27.9 (±10.0)	3.7 (±1.4)	1.5 (±0.3)	14.4 (±3.7)	2.1 (±0.2)
	20.0/38.0	16.8–48.8	1.8/7.2	1.1/2.0	8.0/22.0	1.6/2.5
HNS (n = 28)	23.8	27.5 (±6.1)	3.1 (±0.6)	1.0*	8.5 (±3.6)	1.6 (±0.4)
	18.5/28.3	16.0/42.8	0.1/3.8	0.6/1.9	3.0/18.0	0.5/2.4

Note: Minimum/maximum values are given below each unit of central tendency. Units are in millimetres, n = number of mussel plots sampled within each ecoregion.

Abbreviations: NAPF, North American Pacific Fjordland; GUAY, Guayaquil; HWS, Humboldtian wide-shelf; HNS, Humboldtian narrow-shelf.

(algae) for transport back to a field-based laboratory, where they were identified to the lowest taxonomic classification possible using identification keys and the available regional reference materials (Dawson et al., 1964; Howe, 1914; Kozloff & Price, 1987; Romero, 2002). Additional information on the identification of polydorid species including a possible invasive polychaete can be found in Appendix A.

2.3 | Calculating the stratum index of mussel layers

The mussel matrices that were sampled from the intersections of the transects were used for calculating the stratum index of each respective plot. Mussels were measured lengthwise to the nearest 0.5 mm using a Vernier calliper starting with the mussels that served as the centre of attachment followed by mussels attached to the central mussel >1.5 mm in length (dead mussel shells and empty shells were discarded) for a total of $n = 15$ per plot. Mussels <1.5 mm were considered to recruit and can cause a skew in the population data (Guiñez & Castilla, 1999). For each mussel plot, the appropriate unit of central tendency was calculated based on the distribution of the variables shell length (L) and matrix depth (M). The total area under the matrix (total occupation area (S), Hosomi (1985) for shell lengths equal to or greater than 10 mm in length was calculated according to the formula:

$$S = (L \times 0.1587)2$$

and for shell lengths less than 10 mm in length according to the formula:

$$S = (L \times 0.555)1.44$$

The results from the calculations from each of the raw shell lengths were summed using the formula:

$$S = 0.555 \sum ni = 1\ L1.44 \times phi + 0.1587 \sum mi = n + 1\ L2 \times phi$$

where phi is a ratio used to measure body proportions in plants and animals, and phi = 1.6180339887495 (Hosomi, 1985). The summed values were used to represent the variable stratum index (SI) for each corresponding plot (Guiñez & Castilla, 1999; Hosomi, 1987). The distribution of the values for shell length (L), matrix depth (M), stratum index (SI) and species richness values calculated for all plots in this study were evaluated for normal distributions with the Anderson–Darling test ($p > .05$). We calculated mean for observed species richness (S_{obs}) and Shannon–Wiener diversity (H) using randomized re-sampling with bootstrapped standard deviations (SD) from algorithms provided in EstimateS software version 9.1 (Gotelli & Colwell, 2011).

2.4 | Statistical analysis

We sought to use several measures of diversity that would account for the number of species, abundance and evenness that would allow us to explore multiple dependent variables in our analysis. We used Menhinick's (D) index as one of the species diversity measures because this method accounts for abundance in a sample and effectively compares samples of different sizes (Menhinick, 1964). The formula is D = S /√N, where N = the number of individuals sampled and S is the observed species richness; and Shannon–Wiener diversity index ∑ pi ln(pi) (Shannon, 1948), where pi = the relative abundance of individuals for each species. Because shell length was used to calculate the stratum index, we standardized the independent variables in order to adjust for collinearity (Allen, 1997) using the formula:

$$\sigma = \sqrt{\frac{1}{N}\sum_{i=1}^{N}(x_i - \mu)^2}$$

Frequency distributions for all of the variables were analysed for normality using the Anderson–Darling test.

Linear mixed effects and linear effects modelling were performed on the mussel plot data with stratum index, matrix depth, and shell length as the fixed effects, Mehinick's richness (D), and Shannon–Wiener diversity (H') as the response variables, and ecoregion and/or site as the random effects. Akaike information criteria (AIC) scores were calculated for each model to determine the random effects that were the best fit; lower AIC scores indicated the better model (Akaike, 1974). The linear mixed effect model (LMEM) we used is a random-slope/random-intercept model, which measures the variation in the fixed effects versus the response variables for random effects (Bates et al., 2015) using the following formula:

lmer (dependent variable~independent variable + (1|random effect))

To provide a visualization of fixed effects on diversity, independent variables from LMEM models that resulted in statistically significant results ($p < .05$) were then modelled using linear effects (LEM) with the random intercept/fixed slope formula:

lmer (dependent variable~independent variable + (1|random effect 1) + (1|random effect 2)) and plotted using the ggPlot package to show a random intercept and fixed slope plot (Wickham, 2011), for comparison among ecoregions. All linear effects modelling was performed using the lmerTest (Kuznetsova et al., 2017) in R 4.0.2 (R Core Team, 2021) using RStudio v.1.3.1093 (RStudio Team, 2009). Coefficient estimates (variances), standard errors, conditional r-squared (r2c) and statistical significance (Pr<|t|) were reported for the LMEM and the LEM (Paesch et al., 2014).

3 | RESULTS

3.1 | Macro-scale patterns of intertidal benthic species

A total of 72 species representing 12 phyla were found in mussel plots in the NAPF ecoregion; 9 species from 5 phyla were found within the GUAY ecoregion, 49 species from 12 phyla were found

within the HWS ecoregion and 101 species from 11 phyla were found within the HNS ecoregion. Filamentous and foliose green algae were predominantly found in the transects in the GUAY and HNS ecoregions, while corticated red algae were the most predominant in the HWS ecoregion and leathery brown macrophytes were the most predominant in the NAPF ecoregion. Other than mytilids, molluscs were dominant in the GUAY, HWS and HNS ecoregions, followed by arthropods and annelids. Of the molluscs, the limpet *Scurria viridula* was the most common species in the HWS and HNS ecoregions while the periwinkle *Echinolittorina paytensis* was most commonly found in the GUAY ecoregion. Of the arthropods, the barnacle *Jehlius cirratus* was the most commonly found, and among polychaete annelids, *Perinereis* was commonly found in the HWS and HNS ecoregions, followed by a spionid polychaete (*Boccardia* cf. *wellingtonensis*) at Reserva Punta San Juan in the HNS ecoregion. In the NAPF ecoregion, arthropods dominated the mussel plots with *Balanus glandula* as the most commonly found species, followed by *Semibalanus cariosus* and *Amphibalanus* sp., a genus of barnacle known to be invasive in the eastern north Pacific (Carlton et al., 2011). A table of species encountered in the mussel plots by ecoregion and site can be found in Appendix B.

3.2 | Mussel shell length and stratum index as predictors of diversity in mussel aggregations

We tested the appropriateness of mussel matrices' physical characteristics in predicting species diversity. A total of 89 mussel plots were sampled, with a total of 89 mussel matrix replicates sampled for the biodiversity analysis, and 1118 mussels were measured lengthwise to calculate the stratum indices. Due to omissions in the sampling of shell lengths in 3 of the 89 plots, 86 plots were included in the analysis. Summary statistics were calculated for mean values of the fixed effects that had a normal distribution, and the range of values from minimum to maximum for stratum index, matrix depth and shell length, along with sample size (number of mussel plots sampled) for each respective ecoregion (Table 2).

The lowest AIC scores from the random slope/random intercept LMEM models included ecoregion as the random effect and site as the nested random effect. The random slope/random intercept LMEM produced significant effects of varying magnitude for the standardized shell length and stratum index across all three diversity measures used, with shell length accounting for most of the variance (Table 3). Satterthwaite's method for approximating degrees of freedom is used by the lmer command to produce *p*-values for the *t*-test with significance at alpha adjusted to ≤0.02 to correct for multiple comparisons that showed significant differences in the S_{obs} model for shell length (estimate = 4.91, $p = .004$), in the D model for shell length (estimate = 0.39, $p = .02$) and the H model for shell length (estimate = 0.18, $p = .0$). The conditional r-squared values indicated that the strength of the relationship of the random and fixed effects for all models was strong; however, when the raw values for shell length and stratum index were analysed individually in the random intercept/fixed slope LEM model, only shell length was significant for variation in both richness S_{obs} (Est. =0.20, $p = .02$) and richness D (Est. =0.03, $p = .001$) (Table 4). The slopes for the LEM suggest that S_{obs} increases with increasing shell length, with ecoregion explaining much of the variation. The slopes also suggest that Menhinick's (D) increases with increasing shell length with an increase in the stratum index (with intercepts varying across ecoregions). Although the AIC score for the model of shell length v D is the lowest for both models, the model for stratum index explained most of the variation in D. The results from the LEM suggest that species richness can be predicted from shell length and stratum index with regional variation (Figure 2).

4 | DISCUSSION

Shell size, matrix depth and the complexity of mussel aggregations are linked to age class and various environmental factors that exist where the mussel aggregations are found (Alvarado & Castilla, 1996). Here, we examined the physical geometry of the mussel matrices and their associated benthic macro-scale communities across a broad

TABLE 3 Estimates of variances and standard errors with conditional r-squared from the random slope/random intercept linear mixed models to analyse the effects of matrix depth, shell length and stratum index on species richness (S), Menhinick's richness (D) and Shannon-Wiener (H') diversity in mussel plots sampled from the GUAY, HWS, HNS and NAPF ecoregions.

	Species richness (S)			Menhinick's richness (D)			Shannon–Wiener		
	Estimate	SE	Pr(<|t|)	Estimate	SE	Pr(<|t|)	Estimate	SE	Pr(<|t|)
Intercept	10.70	1.42	**<0.001**	1.26	0.12	**<0.001**	1.77	0.14	**<0.001**
Matrix depth	−0.31	0.5	0.53	0.06	0.06	0.33	−0.06	0.05	0.22
Shell length	4.91	1.7	**0.004**	0.39	0.17	**0.02**	0.44	0.16	**0.006**
Stratum index	−2.47	1.2	0.04	−0.16	0.13	0.19	−0.24	0.11	**0.04**
	r2c = 0.71			r2c = 0.60			r2c = 0.74		

Note: Independent variables with collinearity were standardized. Standard deviations of the variances explained by the random effects ecoregion and site were, respectively, 2.42 and 2.30 for (S), 0.20 and 0.18 for (D) and 0.09 and 0.11 for (H'). Satterthwaite's method for approximating degrees of freedom is used by the R, lmer command to produce *p*-values for the t-test, with significance at ≤0.02 (in bold).

TABLE 4 Variances and significant values from the fixed slope/random intercept linear effects (LEM) models of the respective relationships between the fixed effect shell length versus species richness (S) and Menhinick's (D) and stratum index versus (S) and (D), calculated from mussel plots from all ecoregions in this study.

	Species richness (S)				Menhinick's richness (D)				AIC
	Estimate	SE	Pr(<|t|)	r^2_c	Estimate	SE	Pr(<|t|)	r^2_c	
intercept	6.07	2.45	**0.04**		0.57	0.23	**0.03**		
shell length	0.20	0.09	**0.03**	0.68	0.03	0.009	**0.003**	0.55	80.57
intercept	8.76	2.37	**<0.001**		0.92	0.23	**<0.001**		
stratum index	0.48	0.40	0.22	0.73	0.10	0.04	**0.03**	0.61	84.69

Note: In these models, the slopes of the dependent variables versus the independent variables are the same among all ecoregions, while the intercepts vary. Of the random effects, ecoregion explained more of the variation than did site for both models (S) and (D) (ss = 3.02 and sD = 0.23). A comparison of the models that demonstrated significance at $p < .05$ (in bold) (shell length vs. D and stratum index vs. D) from the lmer test was performed with a post hoc Chi-squared ANOVA. The two models were significantly different ($p < .001$); corresponding AIC scores are given in the right-hand column of the table.

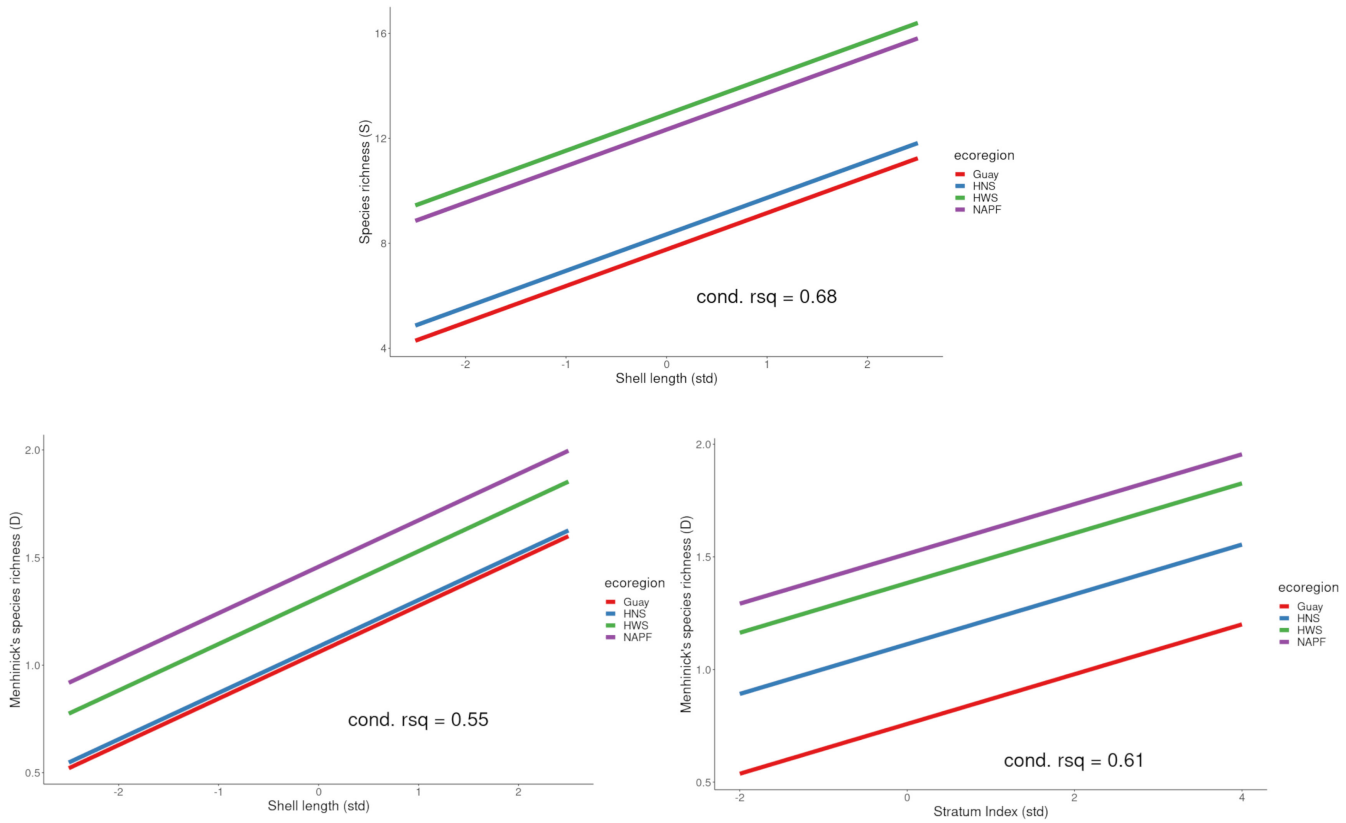

FIGURE 2 Line graphs of the fixed slope/random intercept model from the linear effects modelling (LEM) fixed (shell length and stratum index) and random (ecoregion and site) effects versus species richness for mussel plots sampled from all ecoregions. a) Shell length and observed species richness (S_{obs}); b) shell length and Menhinick's richness (D); and c) stratum index and Menhinick's richness (D). Models were chosen from an alpha <0.05 with the conditional r-squared (fixed and random effects) value provided in the bottom right corner of each graph. Each ecoregion is represented by the coloured line indicated in the legend. Abbreviations for each ecoregion are as follows: GUAY = Guayaquil, HNS = Humboldtian Narrow-shelf, HWS = Humboldtian Wide-Shelf and NAPF = North American Pacific Fjordland.

ecoregional scale in an effort to better understand the characteristics of mussel matrices, particularly when attempting to predict patterns in diversity. It has been suggested that environmental factors often play a role in the abundance and presence of certain species, and because the marine ecoregions are partly defined by local conditions (Ibanez-Erquiaga et al., 2018; Valqui et al., 2021), "ecoregions" as random effects were incorporated into the modelling analysis. Therefore, our results support small-scale experimental results which show that mussel bed complexity is an important factor in determining species composition and abundance (Koivisto & Westerbom, 2010). Although over time, studies have utilized increasingly complex approaches in an effort to characterize mussel bed structure, for example, chain-length

approaches (Aronson & Precht, 1995), fractal analysis (Commito & Rusignuolo, 2000) or three-dimensional surface rugosity (Parravicini et al., 2006), we suggest that mussel shell length (an individual-based measure) is potentially the most important component of mussel bed complexity and can be used as a biomarker for predicting species richness in mussel matrices across different marine ecoregions. That perhaps is not surprising as shell length is an important component of SI, but also perhaps shell length is a strong indicator of shell surface area available to epifaunal organisms. Larger mussels are generally older mussels, which suggests a longer period of time for colonization by other species. Furthermore, larger (thus potentially older) mussels are the main locus of attachment for younger, smaller mussels (Commito et al., 2014). As new mussels recruit onto the existing mussels, this leads to an increase in surface area for epifaunal organisms to colonize on, as well as increasing the spatial complexity, which may lead to a further increase in species richness. While species richness (S_{obs}) may have a stronger positive correlation with shell length, species richness (D) may be predicted with a higher level of precision based on model parameters.

Our study has demonstrated that species richness is higher in multi-layered matrices regardless of whether the matrix is defined by the depth or by the more complicated stratum index formula, suggesting that by providing more habitable substrate, the surface area of the matrix may be a function of species richness. This result is confirmed by other studies that suggest that mussel bed complexity is a more important aspect in determining levels of diversity compared to the availability of nutrients, indicating perhaps a more top-down effect of community composition than a bottom-up one (Firstater et al., 2011). Along the same lines, it has been shown that invasive mussel species that contribute to an increase in mussel bed complexity contribute to an increase in diversity, more so than native mussel species (Gestoso et al., 2013). Here, we show the importance of stratum index as a predictor of community heterogeneity within mussel matrices. Prado and Castilla (2006) recognized the relevance of a stratum index for defining environmental complexity in mussel matrices and utilized matrix depth as an appropriate field method for quantifying mono- and multi-layered matrices. We have shown that measuring matrix depth in the field was indeed found to be an efficient method for describing matrix layers, nevertheless, calculating the stratum index is useful due to the incorporation of area and shell length, both of which assist in determining the level of structural complexity and predominant age class of the mussels. Here, we have successfully recruited these easily observational factors (matrix depth and shell length) as well as the formula for stratum index developed by Hosomi (1985) to demonstrate its usefulness for predicting species richness in complex mussel aggregations in the four ecoregions under study.

ACKNOWLEDGMENTS

Appreciations are due to the staff members of the Reserva Punta San Juan and the Center for Environmental Sustainability of Universidad de Cayetano Heredia in Lima Peru for their assistance with permitting and fieldwork, to the Ministero de la Producción de Peru for the permit to collect marine specimens, the Servicio Nacional de Áreas Naturales for permission to work in the Reserve, Shaleyla Kalez of EcoOceanica for her assistance with logistics in the northernmost ecoregion of Peru and Prof. Aldo Pacheco from the Universidad de Cayetano for his assistance with logistics and species identification in Antofagasta Chile (Bruno Ibaniez-Erquiaga MSc (UPCH) for his assistance in the field). This study was partially supported by the University of Aberdeen, School of Biological Sciences. We would also like to thank the MASTS pooling initiative (The Marine Alliance for Science and Technology for Scotland). MASTS is funded by the Scottish Funding Council (grant reference HR09011) and contributing institutions. The authors declare no conflict of interest. Data are available from authors at request.

DATA AVAILABILITY STATEMENT

Data available from authors at request.

ORCID

Frithjof C. Küpper https://orcid.org/0000-0003-1273-7109
Vasilis Louca https://orcid.org/0000-0001-9560-0479

REFERENCES

Akaike, H. (1974). A new look at the statistical model identification. *IEEE Transactions on Automatic Control*, *19*, 716–723.

Allen, M. P. (Ed.). (1997). Regression analysis with standardized variables. In *Understanding Regression Analysis* (pp. 46–50). Springer.

Alvarado, J. L., & Castilla, J. C. (1996). Tridimensional matrices of mussels Perumytilus purpuratus on intertidal platforms with varying wave forces in Central Chile. *Marine Ecology Progress Series*, *133*, 135–141.

Aronson, R. B., & Precht, W. F. (1995). Landscape patterns of reef coral diversity: A test of the intermediate disturbance hypothesis. *Journal of Experimental Marine Biology and Ecology*, *192*(1), 1–14.

Bateman, D. C., & Bishop, M. J. (2017). The environmental context and traits of habitat-forming bivalves influence the magnitude of their ecosystem engineering. *Marine Ecology Progress Series*, *563*, 95–110.

Bates, D., Mächler, M., Bolker, B., & Walker, S. (2015). Fitting linear mixed-effects models using lme4. *Journal of Statistical Software*, *67*, 1–48. https://doi.org/10.18637/jss.v067.i01

Blake, J. A., & Kudenov, J. D. (1978). The Spionidae (polychaeta) from southeastern Australia and adjacent areas with a revision of the genera of the family. *Memoirs of Museum Victoria*, *39*, 171–280. https://doi.org/10.24199/j.mmv.1978.39.11

Buhl-Mortensen, L., Vanreusel, A., Gooday, A. J., Levin, L. A., Priede, I. G., Buhl-Mortensen, P., Gheerardyn, H., King, N. J., & Raes, M. (2010). Biological structures as a source of habitat heterogeneity and biodiversity on the deep ocean margins. *Marine Ecology*, *31*(1), 21–50.

Carlton, J. T., Newman, W. A., & Pitombo, F. B. (2011). Barnacle invasions: Introduced, cryptogenic, and range expanding Cirripedia of North and South America. In *In the wrong place-alien marine crustaceans: Distribution, biology and impacts* (pp. 159–213). Springer.

Çinar, M. E. (2013). Alien polychaete species worldwide: Current status and their impacts. *Journal of the Marine Biological Association of the United Kingdom*, *93*(5), 1257–1278.

Cole, V. J. (2009). Densities of polychaetes in habitat fragments depend on the surrounding matrix but not the complexity of the remaining fragment. *Austral Ecology*, *34*(4), 469–477.

Commito, J. A., Commito, A. E., Platt, R. V., Grupe, B. M., Piniak, W. E. D., Gownaris, N. J., Reeves, K. A., & Vissichelli, A. M. (2014).

Recruitment facilitation and spatial pattern formation in soft-bottom mussel beds. *Ecosphere*, *5*(12), 1–26.

Commito, J. A., Como, S., Grupe, B. M., & Dow, W. E. (2008). Species diversity in the soft-bottom intertidal zone: Biogenic structure, sediment, and macrofauna across mussel bed spatial scales. *Journal of Experimental Marine Biology and Ecology*, *366*(1–2), 70–81.

Commito, J. A., & Rusignuolo, B. R. (2000). Structural complexity in mussel beds: The fractal geometry of surface topography. *Journal of Experimental Marine Biology and Ecology*, *255*(2), 133–152.

Dawson, Y. E., Acleto, C., & Foldvik, N. (1964). *The seaweeds of Peru*. Beihefte zur Nova Hedwigia.

Engle, J. M. (2008). *Unified monitoring protocols for the multi-agency rocky intertidal network*. University of California, Santa Barbara, CA, USA.

Firstater, F. N., Hidalgo, F. J., Lomovasky, B. J., Ramos, E., Gamero, P., & Iribarne, O. O. (2011). Habitat structure is more important than nutrient supply in modifying mussel bed assemblage in an upwelling area of the Peruvian coast. *Helgoland Marine Research*, *65*(2), 187–196.

Fosberg, F. R. (1976). A classification of the biogeographical provinces of the world, by MDF Udvardy.(IUCN occasional paper 18.) International Union for Conservation of nature and natural resources, Morges, Switzerland: 49 pp., maps, 29$\times$ 20$\times$ 0.4 cm (mimeogr., no price indicated), 1975. *Environmental Conservation*, *3*(4), 313–314.

Gestoso, I., Arenas, F., Rubal, M., Veiga, P., Peña, M., & Olabarria, C. (2013). Shifts from native to non-indigenous mussels: Enhanced habitat complexity and its effects on faunal assemblages. *Marine Environmental Research*, *90*, 85–95.

Gotelli, N. J., & Colwell, R. K. (2011). Estimating species richness. In *Frontiers in measuring biodiversity; Magurran*, *AE & McGill*, *BJ*. Oxford University Press.

Guiñez, R., & Castilla, J. C. (1999). A tridimensional self-thinning model for multilayered intertidal mussels. *The American Naturalist*, *154*(3), 341–357.

Günther, C.-P. (1996). Development of small Mytllus beds and its effects on resident intertidal macro fauna. *Marine Ecology*, *17*(1–3), 117–130.

Hammond, W., & Griffiths, C. (2006). Biogeographical patterns in the fauna associated with southern African mussel beds. *African Zoology*, *41*(1), 123–130.

Hilbish, T., Carson, E., Plante, J., Weaver, L., & Gilg, M. (2002). Distribution of Mytilus edulis, M. galloprovincialis, and their hybrids in open-coast populations of mussels in southwestern England. *Marine Biology*, *140*(1), 137–142.

Hosomi, A. (1985). On the persistent trend of constant biomass and the constant total occupation area of the mussel Mytilus galloprovincialis (Lamarck). *Venus (Japanese Journal of Malacology)*, *44*(1), 33–48.

Hosomi, A. (1987). On the density effect in populations of the mussel Mytilus Galloprovincialis. *Venus (Japanese Journal of Malacology)*, *46*(2), 116–126.

Howe, M. A. (1914). *The marine algae of Peru* (Vol. *15*). Press of the New era printing Company.

Ibanez-Erquiaga, B., Pacheco, A. S., Rivadeneira, M. M., & Tejada, C. L. (2018). Biogeographical zonation of rocky intertidal communities along the coast of Peru (3.5–13.5 S Southeast Pacific). *PLoS One*, *13*(11), e0208244.

Jaramillo, E., Bertrán, C., & Bravo, A. (1992). Community structure of the subtidal macroinfauna in an estuarine mussel bed in southern Chile. *Marine Ecology*, *13*(4), 317–331.

Jones, C. G., Lawton, J. H., & Shachak, M. (1997). Positive and negative effects of organisms as physical ecosystem engineers. *Ecology*, *78*(7), 1946–1957.

Kelaher, B. P. (2003). Changes in habitat complexity negatively affect diverse gastropod assemblages in coralline algal turf. *Oecologia*, *135*(3), 431–441.

Koivisto, M. E., & Westerbom, M. (2010). Habitat structure and complexity as determinants of biodiversity in blue mussel beds on sublittoral rocky shores. *Marine Biology*, *157*(7), 1463–1474.

Kozloff, E. N., & Price, L. H. (1987). *Marine invertebrates of the Pacific northwest*. University of Washington Press.

Krabbenhöft, A., Bialas, J., Kopp, H., Kukowski, N., & Hübscher, C. (2004). Crustal structure of the Peruvian continental margin from wide-angle seismic studies. *Geophysical Journal International*, *159*(2), 749–764.

Kuznetsova, A., Brockhoff, P. B., & Christensen, R. H. B. (2017). lmerTest package: Tests in linear mixed effects models. *Journal of Statistical Software*, *82*(13), 1–26. https://doi.org/10.18637/jss.v082.i13

Lee, M. R., & Castilla, J. C. (2012). Do changes in microhabitat availability within a marine reserve reduce the species richness of small mobile macrofauna and meiofauna? *Journal of the Marine Biological Association of the United Kingdom*, *92*(6), 1283–1288.

Menhinick, E. F. (1964). A comparison of some species-individuals diversity indices applied to samples of field insects. *Ecology*, *45*(4), 859–861.

Paesch, L., Norbis, W., & Inchausti, P. (2014). Effects of fishing and climate variability on spatio-temporal dynamics of demersal chondrichthyans in the Río de la Plata, SW Atlantic. *Marine Ecology Progress Series*, *508*, 187–200.

Paquette, L., Archambault, P., & Guichard, F. (2019). From habitat geometry to ecosystem functions in marine mussel beds. *Marine Ecology Progress Series*, *608*, 149–163.

Parravicini, V., Rovere, A., Donato, M., Morri, C., & Bianchi, C. N. (2006). A method to measure three-dimensional substratum rugosity for ecological studies: An example from the date-mussel fishery desertification in the North-Western Mediterranean. *Journal of the Marine Biological Association of the United Kingdom*, *86*(4), 689–690.

Prado, L., & Castilla, J. C. (2006). The bioengineer Perumytilus purpuratus (Mollusca: Bivalvia) in Central Chile: Biodiversity, habitat structural complexity and environmental heterogeneity. *Journal of the Marine Biological Association of the United Kingdom*, *86*(2), 417–421.

R Core Team. (2021). *R: A language and environment for statistical computing*. R Foundation for Statistical Computing. https://www.R-project.org/

Read, G. B. (1975). Systematics and biology of polydorid species (polychaeta: Spionidae) from Wellington harbour. *Journal of the Royal Society of new Zealand*, *5*(4), 395–419.

Romero, O. Z. (2002). *Guía de biodiversidad N 1 Macrofauna y Algas Marinas Moluscos*, *Centro Regional de Estudios de Educación Ambiental (CREA) Proyecto Mecesup Ant* (p. 77). Antofagasta.

RStudio Team. (2009). *RStudio: Integrated development for R*. RStudio, PBC.

Sato-Okoshi, W., & Takatsuka, M. (2001). Polydora and related genera (polychaeta, Spionidae) around Puerto Montt and Chiloé Island (Chile), with description of a new species of Dipolydora. *Bulletin of Marine Science*, *68*(3), 485–503.

Sepúlveda, R. D., Camus, P. A., & Moreno, C. A. (2016). Diversity of faunal assemblages associated with ribbed mussel beds along the south American coast: Relative roles of biogeography and bioengineering. *Marine Ecology*, *37*(5), 943–956.

Shannon, C. E. (1948). A mathematical theory of communication. *The Bell System Technical Journal*, *27*(3), 379–423.

Simon, C., Worsfold, T., Lange, L., & Sterley, J. (2010). The genus Boccardia (polychaeta: Spionidae) associated with mollusc shells on the south coast of South Africa. *Journal of the Marine Biological Association of the United Kingdom*, *90*(3), 585–598.

Spalding, M. D., Fox, H. E., Allen, G. R., Davidson, N., Ferdaña, Z. A., Finlayson, M., Halpern, B. S., Jorge, M. A., Lombana, A., Lourie, S. A., Martin, K. D., McManus, E., Molnar, J., Recchia, C. A., & Robertson, J. (2007). Marine ecoregions of the world: A bioregionalization of coastal and shelf areas. *Bioscience*, *57*(7), 573–583.

Strub, P. T. (1998). Coastal Ocean circulation off western South America. In A. R. Robinson & K. H. Brink (Eds.), *The Sea* (Vol. *11*, pp. 273–315). Wiley.

Thiel, M., & Ullrich, N. (2002). Hard rock versus soft bottom: The fauna associated with intertidal mussel beds on hard bottoms along the coast of Chile, and considerations on the functional role of mussel beds. *Helgoland Marine Research*, *56*(1), 21–30.

Tokeshi, M., & Romero, L. (2000). Spatial overlap and coexistence in a mussel-associated Polychaete assemblage on a south American rocky shore. *Marine Ecology*, *21*(3–4), 247–261.

Valqui, J., Ibañez-Erquiaga, B., Pacheco, A. S., Wilbur, L., Ochoa, D., Cardich, J., … others. (2021). Changes in rocky intertidal communities after the 2015 and 2017 El Niño events along the Peruvian coast. *Estuarine, Coastal and Shelf Science*, *250*, 107142.

Wickham, H. (2011). Ggplot2. *Wiley Interdisciplinary Reviews: Computational Statistics*, *3*(2), 180–185.

How to cite this article: Wilbur, L., Küpper, F C., Katsiaras, N., & Louca, V. (2023). Predicting diversity in benthic macro-scale communities associated with mussel matrices in three Pacific ecoregions. *Marine Ecology*, *44*, e12741. https://doi.org/10.1111/maec.12741

APPENDIX A

A.1. IDENTIFICATION OF A POTENTIAL INVASIVE POLYCHAETE SPECIES

In March 2019, during field work at Reserva Punta San Juan in southern Peru, mussels covering a 30×30 cm area were removed from rocky intertidal substrate and placed in a shallow tray of seawater for 30 min to allow Polydorids and other invertebrates to emerge from the mussels. Specimens were collected and fixed in alcohol for transport. Herein, the terminology found in Blake and Kudenov (1978) was followed (Table A.1). During species identification, Polydorids were treated separately due to the possible recording of an invasive species. 12 individuals that were preliminarily identified as belonging to the genus *Boccardia* were examined for the following morphometric characteristics: prostomium shape, presence of notoseta on chaetiger 1, shape of major spine type I, shape of major spine type II, starting chaetiger of bidentate hooded hooks, and the presence of posterior notopodial spines. For analysing the relevant information, an OLYMPUS SZE stereoscope and OLYMPUS BZ43 microscope were used. All the specimens were deposited in the formal Polychaetes Reference Collection of Zoobenthos Lab (Hellenic Centre for Marine Research, Greece).

A.2. TAXONOMIC AND ECOLOGICAL ACCOUNTS OF POSSIBLE INVASIVE SPECIES

The polydorid specimens were identified as *Boccardia* cf. *wellingtonensis* based on the following diagnostic characters: incised prostomium, absence of notoseta in chaetiger 1, chaetiger 5 with major spines of two types: falcate and bristle-topped, bidentate hooded hooks from chaetiger 7 onwards, bidentate throughout, and presence of posterior notopodial spines in the last chaetigers (Figure A.1.).

Our material was found to match all the diagnostic characteristics of *Boccardia wellingtonensis* (Read, 1975), except the presence of posterior notopodial spines, which are not reported for the latter. However, the presence could have been overlooked previously or could be variable in occurrence (J. Blake, pers. com). Therefore, it is regarded herein that the specimens most likely belong to *B. wellingtonensis*. The final confirmation of the identification must be defined in a future re-description of the species, which would be possible after acquiring additional material and examining the type specimen.

The species so far has been recorded across the southern hemisphere, in New Zealand (Read, 1975), Chile (Sato-Okoshi & Takatsuka, 2001) and South Africa (Simon et al., 2010). Also, preliminary identifications from material originally identified as *Boccardia polybranchia* are reported from Australia and Argentina by Simon et al. (2010). It is not regarded as non-indigenous in the areas found (Çinar, 2013). To our knowledge, the material from the present study would constitute the first report from Peru.

Boccardia wellingtonensis is considered a non-boring species (Sato-Okoshi & Takatsuka, 2001). In the present study, specimens were found among mussel beds and muddy deposits in dead shells of *Scurria viridula* (Lamarck, 1819).

Table A.1. Identification information and notes taken of samples of *Boccardia* cf. *wellingtonensis* specimens collected from Reserva Punta San Juan in March 2019.

Sample ID	Vial number	Species (genus)	No. of specimens	Notes
260319-1	9	*Boccardia* cf. *wellingtonensis*	1	1 complete individual, broken into 3 parts (posterior end present)
270319-1	4	*Boccardia* cf. *wellingtonensis*	1	1 anterior fragment and 4 middle fragments, no posterior end
280319-1	1	*Boccardia* cf. *wellingtonensis*	3	very fragile specimens
290319-3	3	*Boccardia* cf. *wellingtonensis*	1	boring dead *Scurria viridula*, fragile specimen
290319-4	7	*Boccardia* cf. *wellingtonensis*	2	2 anterior fragments
2903199-6	5	*Boccardia* cf. *wellingtonensis*	4	4 anterior fragments and 4 middle fragments, no posterior end present

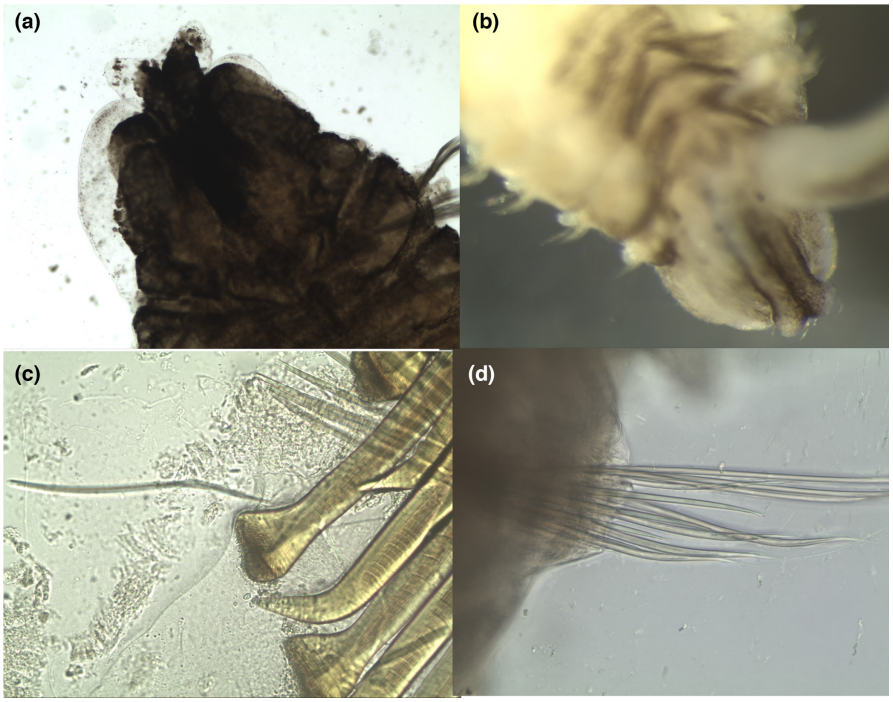

FIGURE A.1 Stereoscopic images of the specimen proposed as the polychaete *Boccardia wellingtonensis* (family Spionidae, Read, 1975) collected from Reserva Punta San Juan in the Marcona district in the Humboldtian ecoregion of Peru. Counter-clockwise from top left, (a)-(b) dorsal view of prostomium, showing the prostomial incision characteristic of *B. wellingtonensis*, (c) bristles visible at the top of spines on setiger 5, and (d) notopodial spines present on last segments.

APPENDIX B

Table B.1. Table of invertebrates and algae encountered in intertidal mussel communities at sites within the Guayaquil (GUAY), Humboldtian Wide-Shelf (HWS) and Humboldtian Narrow-Shelf (HNS) ecoregions in this study. Site abbreviations are given where particular species were found.

	Guayaquil	Humboldtian wide-shelf			Humboldtian narrow-shelf				
Chlorophyta									
Chaetomorpha firma	ENU								
Ulva rigida	ENU		PFA	PGA	PSJ N5n	PSJ N5s	PSJ S4	PSJ S5	UOA
Ulva lactuca		PEN							
Cladophora coelothrix			PFA	PGA					
Blue-green algae					PSJ N5n	PSJ N5s			
Other green algae undet. sp.					PSJ N5n				
Filamentous algae undet. sp.							PSJ S4		
Ochrophyta									
Petalonia fascia		PEN	PFA				PSJ S4		
Brown micro-algae					PSJ N5n	PSJ N5s			
Rhodophyta									
Hildenbrandia sp.	ENU		PFA						
Ahnfeltia durvillei var. implicata			PFA	PGA				PSJ S5	
Ceramium rubrum		PEN							
Chondracanthus glomeratus		PEN					PSJ S4	PSJ S5	
Filamentous red algae undet. sp.		PEN		PGA					
Gigartina sp.		PEN							
Lithothamnion sp.			PFA	PGA	PSJ N5n				
Corticated red algae undet. sp.			PFA						
Corallina officinalis							PSJ S4		

	Guayaquil		Humboldtian wide-shelf			Humboldtian narrow-shelf				
Chondracanthus chammissoi									PSJ S5	
Red algae undet. sp.									PSJ S5	
Nitophyllum sp.										UOA
Cnidaria										
Phymactis clematis				PFA	PGA					
Anemone undet. sp.								PSJ S4	PSJ S5	
Nematoda										
Nematode undet. sp.			PEN	PFA	PGA	PSJ N5n		PSJ S4		
Platyhelminthes										
Polyclad undet. sp.		ENU	PEN	PFA	PGA			PSJ S4	PSJ S5	
Nemertea										
Nemertean undet. sp.				PFA	PGA		PSJ N5s		PSJ S5	UOA
Annelida										
Phyllodocidae		ENU	PEN							
Glycera sp.			PEN	PFA	PGA			PSJ S4	PSJ S5	UOA
Nereis sp.			PEN	PFA					PSJ S5	
Perinereis sp.			PEN	PFA	PGA			PSJ S4	PSJ S5	UOA
Polynoidae			PEN	PFA	PGA					
Serpulidae				PFA						
Syllidae								PSJ S4	PSJ S5	
Owenidae						PSJ N5n			PSJ S5	
Spionidae						PSJ N5n	PSJ N5s	PSJ S4	PSJ S5	
Hesionidae							PSJ N5s			
Mollusca										
Argopecten sp.				1						
Brachidontes sp.	ACA	ENU								
Echinolittorina paytensis	ACA	ENU					PSJ N5s		PSJ S5	UOA
Siphonaria lessoni		ENU		PFA	PGA				PSJ S5	
Lottia orbignyi				PFA	PGA				PSJ S5	
Echinolittorina peruviana			PEN	PFA	PGA	PSJ N5n	PSJ N5s	PSJ S4	PSJ S5	UOA
Perumytilus purpuratus			PEN	PFA	PGA	PSJ N5n	PSJ N5s	PSJ S4	PSJ S5	UOA
Scurria viridula			PEN	PFA	PGA	PSJ N5n	PSJ N5s	PSJ S4	PSJ S5	UOA
Semimytilus algosus			PEN	PFA	PGA	PSJ N5n	PSJ N5s			
Stramonita haemastoma			PEN		PGA					
Gastropod undet. sp.			PEN	PFA						
Chiton granosus				PFA	PGA			PSJ S4	PSJ S5	UOA
Fissurella sp.					PGA					
Tegula atra						PSJ N5n	PSJ N5s	PSJ S4		
Prisogaster niger								PSJ S4	PSJ S5	UOA
Mussel undet. sp.								PSJ S4	PSJ S5	
Chiton undet. sp.										UOA
Incatella cingulata										UOA
Scurria ceciliana										UOA
Scurria parasitica										UOA
Arthropoda										
Grapsidae								PSJ S4		UOA
Cancridae								PSJ S4		

	Guayaquil		Humboldtian wide-shelf			Humboldtian narrow-shelf				
Isopod			PEN	PFA	PGA			PSJ S4	PSJ S5	
Decapod					PGA					
Decapod (megalops phase)			PEN							
Amphipod 1									PSJ S5	
Amphipod 2					PGA					
Amphipod 3					PGA					
Amphipod 4					PGA					
Balanus trigonus				PFA	PGA					
Jehlius cirratus				PFA	PGA	PSJ N5n	PSJ N5s	PSJ S4	PSJ S5	UOA
Barnacle undet. sp.					PGA					UOA
Ostracod									PSJ S5	
Porcellanidae									PSJ S5	
Notochthamalus scabrosus	ACA	ENU		PFA		PSJ N5n				UOA
Bryozoa										
Bryozoan				PFA						
Porifera										
Encrusting sponge				PFA						

Site abbreviations are as follows: ACA, Playa Acapulco; ENU, El Nuro; PEN, Playa Ensenada; PFA, Playa Farallones; PPA, Playa Palmeras; PSJ, Punta San Juan (with sites N5n, N5s, S4 and S5) UOA, Universidad de Antofagasta.

Table B.2. Table of invertebrates and algae encountered in intertidal mussel communities at sites within the NAPF ecoregion. Site abbreviations are given where particular species were found.

	North American Pacific Fjordland			
Chlorophyta				
Chaetomorpha cartilaginea				WPA
Chaetomorpha sp.	KIS	SBE	PCO	
Cladophora sp.		SBE	PCO	WPA
Ulva intestinalis		SBE		
Ulvaria	KIS		PCO	WPA
Ulva lactuca	KIS	SBE		WPA
Ochrophyta				
Alaria nana	KIS		PCO	WPA
Colpomenia peregrina		SBE		
Ectocarpus sp.	KIS	SBE		
Fucus gardneri	KIS	SBE	PCO	WPA
Ralfsia sp.				WPA
Sctyosiphon lomentaria			PCO	WPA
Rhodophyta				
Calliarthron tuberculosum				
Ceramium sp.	KIS			
Corallina frondescens				
Endocladia muricata	KIS	SBE		
Hildenbrandia sp.		SBE		
Mastocarpus sp.				
Mazzaella sp.		SBE		
Microcladia borealis			PCO	

North American Pacific Fjordland				
Odonthalia floccosa	KIS		PCO	
Pterosiphonia bipinnata	KIS	SBE	PCO	WPA
Plocamium violacea			PCO	
Polysiphonia hendryi		SBE	PCO	
Polysiphonia hendryi var.	KIS	SBE		WPA
Halosaccion glanduliforme		SBE	PCO	
Nemalion helminthoides				WPA
Cnidaria				
Anthopleura xanthogrammica			PCO	
Metridium senile	KIS			
Nematoda				
nematode not det.		SBE		WPA
Platyhelminthes				
polyclad not det.	KIS			WPA
Nemertea				
Emplectonema gracile	KIS	SBE	PCO	WPA
nemertean not det.	KIS			WPA
Annelida				
Glycera not det.	KIS			
Nereis sp.	KIS	SBE	PCO	WPA
Cirratulidae not det.				WPA
Mollusca				
Hiatella arctica	KIS			
Littorina scutulata	KIS	SBE	PCO	WPA
Littorina sitkana		SBE	PCO	WPA
Lottia asmi		SBE	PCO	WPA
Lottia digitalis	KIS	SBE	PCO	
Lottia ochracea	KIS	SBE		WPA
Lottia paradigitalis	KIS	SBE	PCO	WPA
Lottia pelta		SBE		WPA
Lottia scutum	KIS			
Lottia sp. not det.		SBE		
Nucella ostrina		SBE		
Mytilus species complex	KIS	SBE	PCO	WPA
Arthropoda				
Balanus glandula	KIS	SBE	PCO	WPA
Amphibalanus sp.	KIS	SBE	PCO	WPA
Semibalanus cariosus	KIS	SBE	PCO	WPA
Chthalamus dalli		SBE		
Balanus crenatus		SBE		WPA
Chromopleustes oculatus	KIS			
amphipod not. det.		SBE		
Idotea wosnesenskii				WPA
isopod not det.	KIS	SBE		
decapod, megalops phase	KIS	SBE		
Cirolana harfordi	KIS	SBE		WPA

Pagurus hirsutiusculus	SBE		
Neomolgus littoralis	SBE		WPA
mite not det.	SBE		WPA
Echinodermata			
Cucamaria sp.		PCO	
Chordata			
solitary tunicate not det.			WPA

Site abbreviations are as follows: KIS, Kayak Island; SBE, Sage Beach; PCO, Pirate's Cove; WPA, Whale Park.